Source Mechanism—Dipole versus Single Force Application to Mining Induced Seismic Events in Deep Level Gold Mines in South Africa

J. Šílený Geophysical Institute, Academy of Sciences, Czech Republic
A.M. Milev CSIR Mining Technology, South Africa

The traditional double-couple source model defined as the force equivalent of a shear slip along a planar fault and widely accepted in earthquake seismology is not always applicable in mining conditions. The general dipole source model is more suitable because it contains the isotropic part and the linear dipoles. The presence of these components can well describe explosions and collapse of cavities. However, the mechanism of some mining-induced seismic events can deviate even from the dipole model. The equivalent single force model is used then to describe these events. A unified methodology to determine the parameters of both dipole and single force model is proposed using the inversion of waveforms generated by mining induced seismic events. Preference of the dipole or single force source model is assessed on the basis of stability of the orientation of the source retrieved, in turn, from both P and S waveforms, and from P waveforms alone. This methodology is demonstrated on inversion of far-field records from mining induced seismic events located in deep level gold mines in South Africa.

1 INTRODUCTION

The mechanism is one of the basic characteristics of a seismic source, since it describes the force system acting in the focal zone. The physics of the process may be different, ranging from fracturing of the originally intact material through creating defects in, for example, civil engineering structures, through slipping along pre-existing faults in large-scale view on most tectonic earthquakes, to fracturing phenomena on complexes of highly stressed areas in underground mining structures, accompanied by slip along local tectonic structures, tensile fracturing at the tips of the discontinuities, and collapsing of void cavities.

Apart from the physics involved, the processes can be described phenomenologically in the unified frame by using the concept of a stress glut introduced by Backus and Mulcahy (1976a,b) and its expansion into polynomial moments by Backus (1977a,b). In the practice of earthquake seismology only the first-degree moment is used, which is the so-called seismic moment tensor. It represents a general dipole source, i.e. a phenomenon generating seismic waves, which is equivalent to force couples acting in the focal zone.

The moment tensor analyses using mining induced seismic events reported by McGarr (1992) used the relationship between the trace of the moment tensor (calculated from the diagonal elements) and the coseismic volume change. More recently Andersen (2001) and Andersen and Spottiswoode (2001) introduced a hybrid moment tensor inversion methodology. This technique attempts to compensate for various types of systematic error that influence seismograms recorded underground in order to achieve a robust measure of the moment tensor. The method is designed to enhance the accuracy of the computed moment tensors by decreasing the influence of any low quality observations, to damp (or amplify) any signals that have been overestimated (or underestimated) due to local site effects, and to correct for raypath focussing or defocussing that results from inhomogeneities in the rockmass (Andersen, 2001).

The most frequent dipole combination used in earthquake seismology is the Double Couple (DC) which consists of two force couples with mutually opposite moments so that their total moment vanishes or, equivalently, two perpendicular force couples without moments. Burridge and Knopoff (1964) derived that the DC is the force equivalent of a shear slip along a planar fault. However, there are more components in seismic Moment Tensor (MT) than a pure DC. The MT decomposition itself is not unique (more exactly, decomposition of the deviatoric part of the MT), but there is a single one which is most commonly used, namely MT decomposition into an isotropic component (ISO), DC and a Compensated Linear-Vector Dipole (CLVD). The latter is a force system consisting of 3 couples without moments along the principal axes of the MT, one of which is along the pressure P-axis or tension T-axis, and the remaining two perpendicular and half in size (Figure 1).

The non-DC components can be real, reflecting displacements in the focal zone differing from the shear slip, e.g. tensile cracking caused by magma or fluid injection in volcanic earthquakes or man-made seismic events induced by hydraulic fracturing of oil and gas wells etc. A comprehensive overview of phenomena characterized by non-DC mechanisms can be found in Julian et al. (1998) and Miller et al. (1998).

On the other hand, however, non-DC components may be spurious, i.e. may be generated as artefacts of an ill-posed inverse task: (i) They may arise as the consequence of using an incorrect model of the source, e.g. the neglect of the bending of a shear fault results in additional CLVD components instead of the pure DC corresponding the shear slip (Frohlich 1984); (ii) They may appear due to mislocation of the hypocenter and, especially; (iii) as the consequence of mismodeling of the medium between the focus and seismic stations (Kuge and Lay, 1994). For example, Šílený and Vavryčuk (2000, 2002) demonstrated appearance of a spurious CLVD caused by neglecting the anisotropy in the focal zone. Šílený et al. (2001) showed the combined effect of hypocenter mislocation and neglecting a reflecting interface near the source.

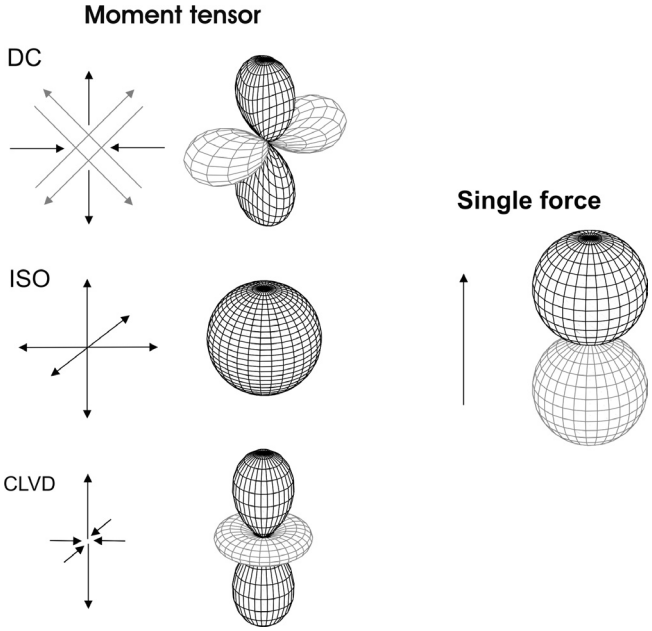

FIG. 1 **Moment tensor vs. single force: force diagram systems (left), and P-wave radiation pattern (right). The moment tensor is decomposed into a double-couple (DC), isotropic component (ISO), and compensated linear-vector dipole (CLVD). Two equivalent force systems are displayed in DC diagram: two couples without moment (black arrows), and two couples with mutually opposing moments (grey arrows). In the radiation pattern diagrams: positive amplitudes – black, negative amplitudes – grey**

In inner sources, where a dislocation is created due to critical stress loading, the total force exerted by the source is zero and the expansion of the seismic response starts with the 1st term corresponding to the seismic moment tensor. There are however, seismogenic processes where a mass advection takes place, like magma flow or landslides, for which the description by the zero-term of the expansion – a single force – is adequate. Takei and Kumazawa (1994, 1995) pointed out that the single force should not be a priori excluded as a seismic source and derived theoretical models of sources with mass advection.

Typical representatives of this class of source are seismic phenomena related to magma flow caused by inflation and deflation of magma chambers, or volcanic eruptions (Kanamori and Given 1982; Kanamori et al. 1984; Nishimura 1995; Brodski et al., 1999). Violation of the moment tensor source model for landslides was observed by Eissler and Kanamori, 1987; Hasegawa and Kanamori, 1987; Kavakatsu, 1989 and correlation of the force direction in the single force model with the direction of landslide was found. Dahlen (1993) derived the single force representation of shallow landslides theoretically. Efficiency of the single force in the excitation of seismic and tsunami waves was pointed out by Okal (1990) and Takei and Kumazawa (1995).

Frequent deviations from a DC-type seismic radiation have been observed in the mines (Rudajev and Šílený, 1985; Wang and McGarr, 1990, Stickney and Sprenke 1993). Usually it has been explained by considering an additional component in the frame of the MT model (Wong et al., 1989; Feignier and Young, 1992; Baker and Young, 1997). A single force model however, should not be excluded a priori for some of them, as a mass advection can take place there; e.g., a collapse of the hangingwall in underground mining conditions (Hasegawa et al. 1989).

The goal of this study is to verify the relevance of both the moment tensor and single force model to strong mine induced seismic events. In this work we will also try to formulate criteria of preference for each source type on the basis of far-field low-frequency waveform inversion.

2 SEISMIC DATA

Seismic data recorded at Driefontein gold mine 5 Shaft was used in this study (Ferreira, 2004). The seismic events were recorded underground by a mine-wide seismic network consisting of 4.5 Hz geophones installed in the solid rock around the excavations. The summary of the seismic events studied is given in Table 1. The values of the seismic parameters are as given by the processing software used in the mine.

TABLE 1 **Summary of the seismic events inverted in this study**

No	Date &Time	Mag	log Mo [Nm]	Stress drop [MPa]	No Trig.
1	18/09/03 16:01:51	2.5	12.67	1.24	11
2	13/12/03 14:14:49	2.8	12.94	1.68	18
3	20/01/04 20:00:24	2.8	12.91	3.31	24
4	25/01/04 08:05:57	2.6	12.82	1.08	22
5	03/06/04 15:24:25	2.7	12.96	1.12	18

Mo = Seismic moment; Mag = Local magnitude, Trig = No. of triggering stations.

Most stations were situated above the source, leaving the lower focal hemisphere unfavourably covered. Moreover, the azimuthal distribution was rather irregular, making the resulting coverage of the focal sphere sparse (Figure 2).

The estimated velocities of the P and S waves are 6200 and 3650 m/s, respectively. Because the recorded data are too complex to be matched by synthetic seismograms constructed using a homogeneous model, they were filtered

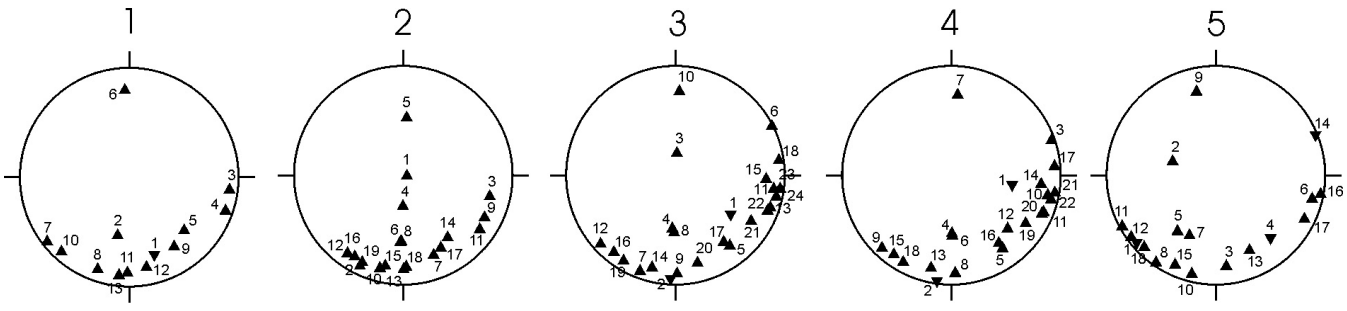

FIG. 2 **Distribution of the station projections onto the focal sphere for the five seismic events summarised in Table 1. The plot is equal-area projection of lower hemisphere of the focal sphere: triangles pointing down are stations below the source; triangles pointing upwards are stations above the source**

using a low-pass filter of five degree and cut-off frequency at 60 Hz. Below this frequency, the response of the instrument seemed to be flat enough. Therefore, there was no need for signal rectification to compensate effect of the instrument. An example of the original waveforms of Event # 1 and the filtered waveforms recorded by stations 1 and 11 is shown in Figure 3.

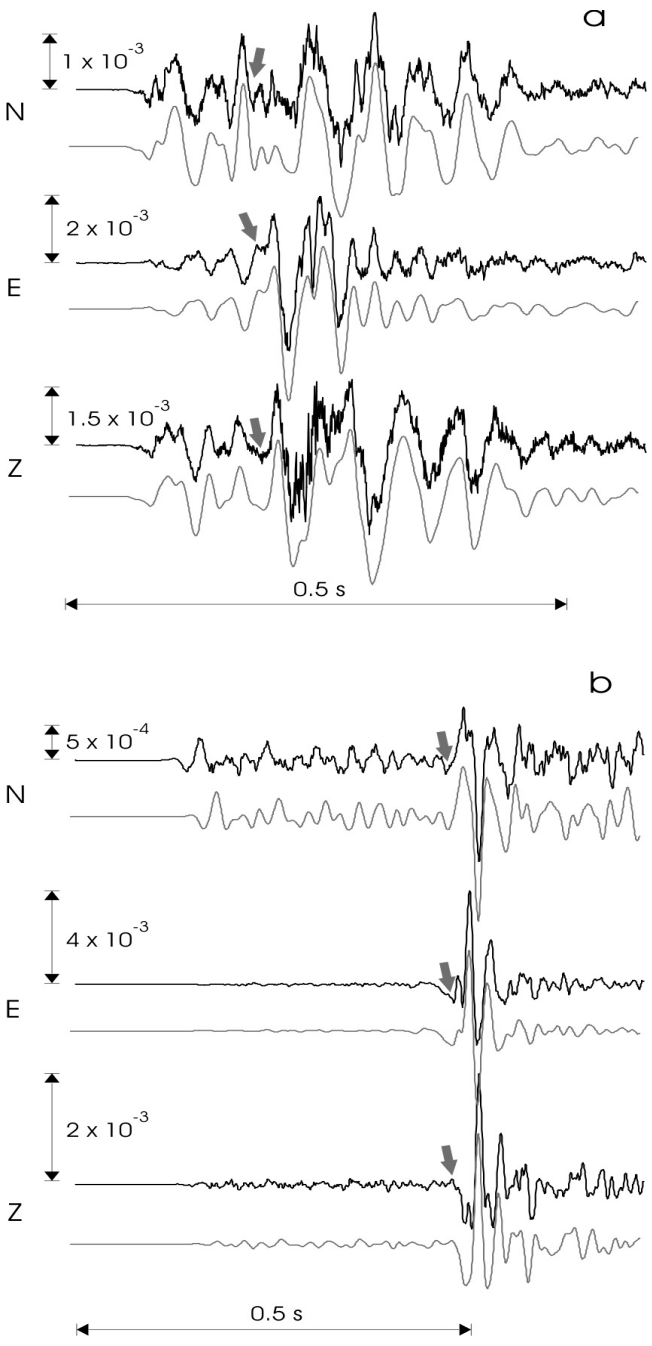

FIG. 3 **Observed (black) and low-pass filtered (grey) velocity records of Event #1 at (a) station 1, hypocenter distance 1143 m, and (b) station 11, hypocenter distance 3373 m. Grey arrow shows the S-wave arrival, velocity in ms^{-1}**

3 METHOD

The INPAR algorithm (Šílený et al. 1992, Šílený 1998) is used to invert the waveforms to retrieve the MT. The source is indirectly parametized: the records are inverted into the Moment Tensor Rate Functions (MTRFs) by the method of optimum filter design by Sipkin (1982), and in the following step the MTRFs are reduced into the MT and the Source Time Function (STF). The unconstrained MT is decomposed into the double couple (DC), isotropic part (ISO), and compensated linear-vector dipole (CLVD). In order to determine parameters of the Single Force (SF) source model, the INPAR algorithm was generalized to proceed from waveforms also through single force time functions corresponding to individual components of the vector of the force to the direction of the single force and the function describing its development in time.

4 SYNTHETIC TESTS

In the theory, distinguishing between MT and SF source models should be straightforward because their radiation patterns are very different for both the P and S waves. For example, contrary to well-known quadrant P-wave radiation pattern of the DC, there are only two lobes in the SF radiation pattern: a positive lobe in the force direction and a negative one against it. The SF radiation pattern is symmetric with respect to a single axis only (coinciding with the force direction), while there are more symmetry axes and a centre of symmetry in the MT radiation pattern. However, the sparse focal sphere coverage makes the separation of the MT from the SF difficult. As the stations are clustered largely in a particular direction, an ambiguity in the separation of MT from SF may be expected when only P waves are inverted. When the station cluster coincides with the positive/negative lobe in the SF radiation pattern, and one of the positive/negative lobes of the MT radiation pattern, the difference in fit of synthetics to the observed data for both models should be small. The resolution should be enhanced by using a complete data set for both P and S waves.

The resolving power of the procedure was tested in a series of synthetic experiments that simulated the station configuration during the 1998 simulated rockburst experiment at Kopanang gold mine (Milev et al. 2001), Figure 4. Similarly, the Driefontein events have very irregular focal sphere coverage and most of the station projections are clustered in the S direction. Synthetic seismograms were generated for the 16 stations of Figure 4 using three types of sources: (1) double couple – vertical strike-slip, striking N; (2) double couple – vertical strike-slip, striking NE, and (3) horizontal single force directed N.

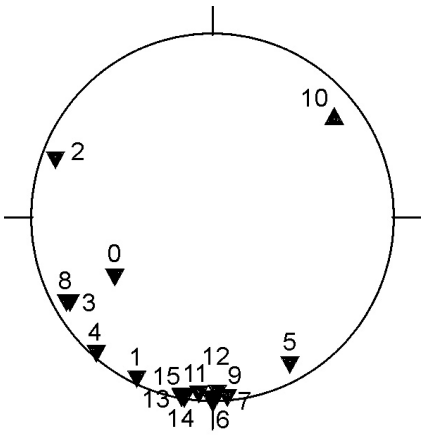

Fig. 4 **Distribution of the station projections onto the focal sphere for the simulated rockburst in the Kopanang mine. For details see the caption of Figure 2**

Additionally, the mismodeling of the source in the waveform inversion problem was modelled. Synthetic data corresponding to the dipole source (1) or (2) were inverted by using the Green's function constructed for the single force source (3) and vice versa. To simulate the situation, the

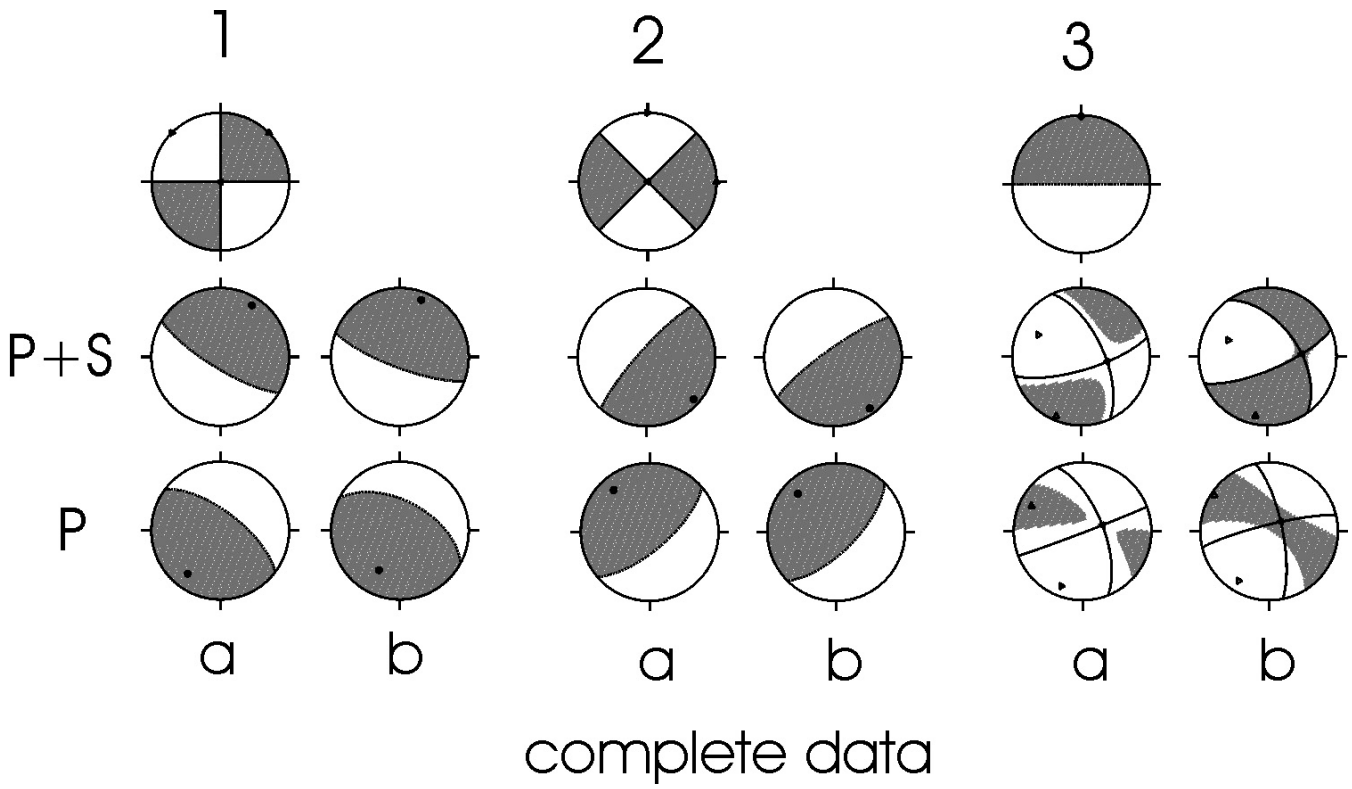

FIG. 5 **Synthetic experiments using a mismodeled source, waveform inversion of data from complete set of stations in Figure 4. Experiment 1: data generated by a moment tensor source – DC: vertical strike-slip striking N, single force model was assumed during the waveform inversion. Experiment 2: data generated by a moment tensor source – DC: vertical strike-slip striking NE, single force model was assumed. Experiment 3: data by single force source (horizontal force directed N), moment tensor model assumed. Vertical annotations: P+S indicates inversion of both P and S waveforms; P is inversion of P-waves only. Horizontal annotations: a is inversion of noise-free data; b is inversion of noisy data. Fault plane solutions of MT and SF sources: solid lines are the nodal lines; grey area is the zone of compressions. The equal-area projection of lower hemisphere is used**

source was erroneously assumed to be of an incorrect type. The objective was to suggest a criterion for recognizing the mistake.

The complete data was inverted using both P and S waves, and then using P-waves only. The data were prepared for the inversion in two ways: (a) as noise-free records, and (b) as noisy data constructed from (a) by adding white noise with random amplitude reaching 50% of the maximum amplitude of the noise-free data. All experiments were performed using two station configurations: (i) complete data, i.e. from all 16 stations, and (ii) reduced data, i.e. stations Nos. 6, 7, 9, 11-15: those, which are tightly clustered near the S pole of the focal hemisphere.

The results of the synthetic experiments are summarized in Figures 5 and 6.

1. In the source reconstructed from both noise-free and noisy P+S data the SF is directed roughly NNE, while the SF calculated using P waves only is steeper having an azimuth of roughly SSW, Figure 5-1a, b. Similarly, after the inversion of the reduced data, the reconstructed SF is consistently directed E for both the noise-free and noisy P and S records, but roughly SW from P records only, Figure 6-1a, b.
2. An analogous pattern is yielded by inverting the complete data set: the reconstructed SF is directed SE for both the noise-free and noisy P+S data, while from the SF calculated from the P data only trends roughly NW. However, the difference in the P and P+S patterns disappears when the reduced station configuration, consisting of stations clustered near the S pole, is used. Both the P and S inversions (for noise-free and noisy data) consistently result in the N direction of the single force, Figures 5-2a,b and 6-2a,b.
3. When all stations are used, both the noise-free and noisy P+S data yields the SF directed N and a MT close to a vertical strike-slip striking NE with nearly horizontal T-axis directed NS, Figure 5-3a,b. However, using the P records only results in a MT with large non-DC components. Once more, the DC part shows nearly horizontal strike-slip striking NEE in the opposite slip direction, where the P-axis is directed NNE-SSW. The reduced data for both P and P+S (and for both noise-free and noisy records) consistently yield roughly 45 degree dip-slip of thrust faulting striking E, where the P-axis is directed NS. There are large non-DC components in the reconstructed MT and dilatations nearly cover the entire the focal sphere, Figure 6 – 3a, b.

The following characteristics can be drawn from the synthetic experiments where the source type was mismodelled:

- In the first and the second experiment, there is a well-pronounced relationship between the direction of reconstructed SF and the DC orientation of the true source if inverted from P-waves. The first experiment satisfies the expectation that the SF should point towards the T-axis if the stations are situated prevailingly in the sector of compressions. In this case, the stations are mostly in the third quadrant and near the S pole of the focal sphere, therefore the SF is identified with the T-axis pointing SW Figure 5-1a, b-P. With the reduced set of stations, the clustering is

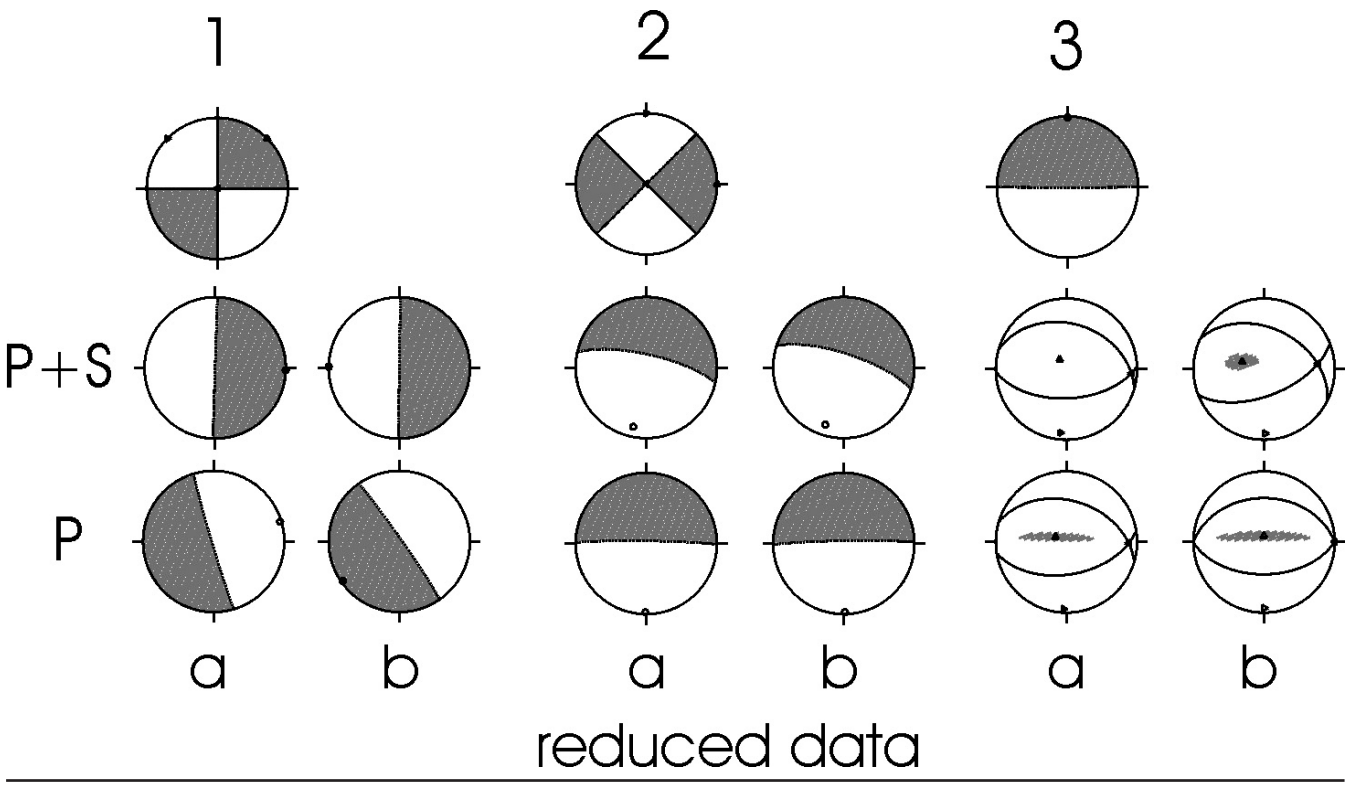

FIG. 6 **Synthetic experiments with mismodeling of the source, waveform inversion of data from reduced set of stations from Fig. 4: only data from stations 6,7,9,11-15 used (i.e. the stations clustered in the S pole of the focal sphere). For details see the caption of Fig. 5**

extreme and the coincidence appears again, Figure 6-1a,b-P. In the second experiment the zone of tightly clustered stations is situated in the zone of dilatations. Therefore, for the reduced set of stations, the resulting SF points against the P-axis at the S pole of the focal sphere, Figure 6-2a,b-P. With the complete set of stations, the rule is violated, Figure 5-2a, b-P.

- The third experiment illustrated the coincidence: the SF of the true source pointing N causes dilatations around the S pole of the focal sphere where most stations are clustered. The reconstructed MT source model displays a P-axis directed SSW and S for both the complete and reduced data, Figure 5-1a,b-P and Figure 6-1a,b-P, respectively. This fits with the pattern.
- When inverting the P+S data, this coincidence is violated, as it is based on partial similarity of P-radiation pattern for SF and suitably inclined DC. This correlation is annihilated when the S waves are added.
- Comparing the orientation of the reconstructed source, in turn, from P and S waves and then from P waves alone, seems to be a prospective indicator of incompatibility of source model with the data. In all the experiments performed the reconstructed source orientation differs essentially when determined from P+S and from P data only (it flips nearly to the opposite). This is valid for the inversion of the complete data, while for reduced set of stations the P and P+S inputs yield nearly the same results. This suggests that good coverage of focal sphere may be crucial in recognizing the incompatibility of the source model.

5 INVERSION OF SEISMIC DATA

From the experience learned from the synthetic experiments with mismodeling of the source in Section 4, we will search for the indicator of the mismodeling, which is the distinct difference in the source orientation, when the source model is retrieved from P and S waves together and from P waves alone. Therefore, four inversions are performed for each event:

- inversion of P and S waveforms assuming the source model is a moment tensor,
- inversion of P waveforms assuming the moment tensor,
- inversion of P and S waveforms assuming the source model is a single force,
- inversion of P waveforms assuming the single force.

The similarity or dissimilarity of P+S and P solutions will then be observed and on the basis of this comparison the source model for each event will be suggested. Results are summarized in Figure 7.

Event #1: The SF model yields force directions differing roughly by 75 degrees, while the MT model displays a similarity. In the MT solution from P+S the dominant component is a CLVD (76%) along the P-axis, P waveform inversion yields a prevalence of the DC (90%). However, the P-axis direction exhibits a good correspondence – the difference falls below 27 degrees. Therefore, the MT seems to be the preferred source model here.

Event #2: The mechanism recovered from P+S and P waveforms differ largely in both source models. The SF direction differs by 77 degrees. The difference of the P-axis direction in the MT model stays within 51 degrees, but the dominant component – CLVD flips from the P-axis in the P+S inversion to the T-axis in the P inversion. Therefore, there is not enough correspondence in either model, and a preference remains unanswered.

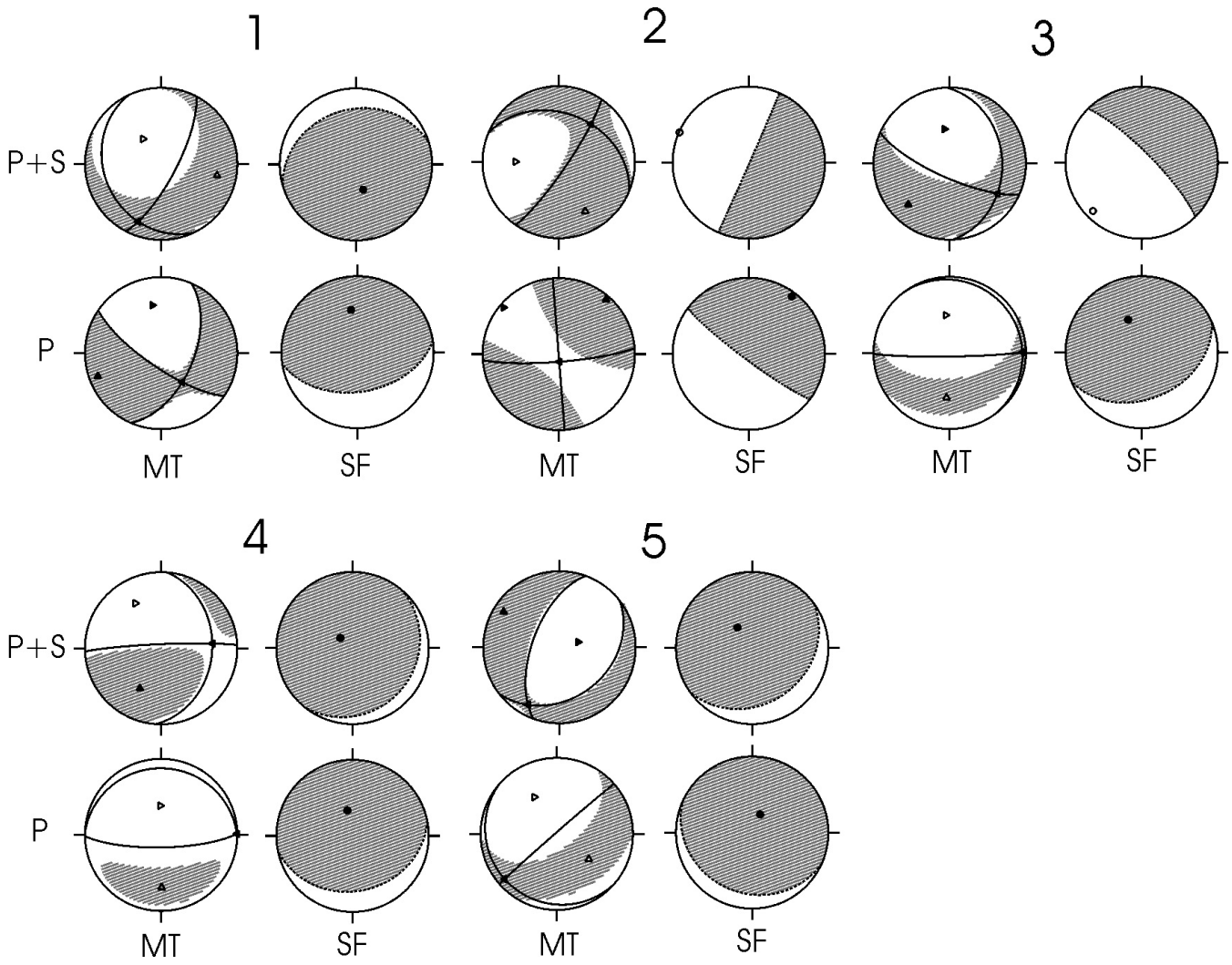

FIG. 7 **Moment tensor vs. single force source models for five seismic events located at Driefontein gold mine: P+S is inversion of both P and S waveforms; P is inversion of P waves only. Fault plane solutions of moment tensor and single force sources: solid lines are nodal planes; grey area is the zone of compressions. The equal-area projection of lower hemisphere is used**

Event #3: Essentially the same pattern as in the Event #1 is observed. The SF direction differs by 85 degrees, in the MT source there is a prevalence of CLVD along P-axis in both P+S and P inversions (52 and 63%, respectively) with the P-axis practically coincident with 4 degrees difference. Therefore, the MT model is preferred here.

Event #4: Retrieved orientations in both source models display good stability for both P+S and P inversions. The SF direction remains within 18 degrees. The MT from P+S is nearly a DC, having only 10% of ISO and 7% of CLVD along the P-axis. There is more CLVD component if determined from P waveforms only, 47% of CLVD is along the P-axis, 29% of ISO. However, the P and T axes do not differ more than about 30 degrees in both cases. Therefore there is no preference for SF or MT models here and both models seem to be plausible.

Event #5: Assuming the MT source model, the T and P axes flip mutually if the P+S and P data are inverted. Alternatively, in the SF model an excellent stability of the force direction is obtained which differs less than 24 degrees. Therefore, the SF source model is preferred in this case.

6 DISCUSSION AND CONCLUSIONS

In earthquake seismology, the single force model has been implicitly excluded from possible source mechanisms, because of the requirement that the mass transfer is balanced in sources represented by a slip along a fault. Unbalanced mass transfer, however, can take place in foci of some of mine induced seismic events, especially those created by gravitational collapse of mined out areas.

Despite the fact that the radiation patterns of a single force and a dipole source are essentially different, in practice, separation of the patterns is difficult due to the usually sparse coverage of the focal sphere by seismic stations. While the P-wave radiation may look similar in a specific direction where the recording stations are clustered, in the S-waves it differs essentially. Therefore, it is reasonable to observe the consistency of the source retrieved either from complete P and S waveforms or from P waves alone, assuming, in turn, the moment tensor and single force model. Synthetic experiments simulating the inversion into a source model incompatible with the data demonstrate the instability of the geometrical characteristics of the source retrieved from P+S and from P waves only. Therefore, we suggest this comparison as a first-approach discrimination tool between the moment tensor and single force source models. The focal

sphere coverage with certain "minimum quality" is however essential. Stations seen from the source within an angle wider than a few tens of degrees should be available.

We applied this approach to five mining induced seismic events located at Driefontein gold mine, South Africa. In turn, P together with S and P waveforms alone filtered by a low-pass filter below 60 Hz were inverted into both moment tensor and single force source models. For two events (Table 1 and Figure 7, #1 and #3) the moment tensor model seems to be more appropriate, having steeply dipping P-axes in both cases. For Event #5 the single-force model is preferred, with the force direction close to vertical. For Event #4 both models seem to be acceptable, and for Event #2 none of them seems to be suitable.

The single-force Event #5 exhibits a force directed very steeply downward. If this model is appropriate for the source, there should be some mass transfer in the focus. The sub-vertical direction of this force may be related to collapse of the hangingwall where the single force model, directed downwards, can be applied.

The approach relies on far-field modelling of the waveforms, which may be rather an over-simplification for events greater than magnitude 2.5 in hypocenter distances of few kilometres. Near-field terms may provide valuable additional constraints to distinguish between the source models discussed. This generalized approach is currently under study.

ACKNOWLEDGMENTS

The Czech Rep. Grant Agency - Grant Project No. 205/02/0383 supported the project. The authors would like to express grateful acknowledgment to Mr Ricardo Ferreira, Gold Fields South Africa for providing the seismic data and to Dr Lindsay Linzer, CSIR Mining Technology for reviewing the manuscript. Comments of the anonymous reviewer suggesting the extension of the analysis are greatly appreciated.

REFERENCES

Andersen, L.M. (2001) A relative moment tensor inversion technique applied to seismicity induced by mining. PhD Thesis, University of the Witwatersrand, South Africa, pp. 230.

Andersen, L.M. and Spottiswoode, S.M. (2001) A hybrid moment tensor inversion methodology. In: Proceedings of the RaSim5 conference (Rockbursts and seismicity in mines), Magaliesberg, South Africa.

Backus, G. (1977) Interpreting the seismic glut moments of total degree two or less, Geophys. J. R. astr. Soc., 51, pp. 1–25.

Backus, G. (1977b) Seismic sources with observable glut moments of spatial degree two, Geophys. J. R. astr. Soc., 51, pp. 27–45.

Backus, G.E. and Mulcahy, M. (1976a) Moment tensors and other phenomenological descriptions of seismic sources I – Continuous displacements, Geophys. J. R. astr. Soc., 46, pp. 341–362.

Backus, G.E. and Mulcahy, M. (1976b) Moment tensors and other phenomenological descriptions of seismic sources II – Discontinuous displacements, Geophys. J. R. astr. Soc., 47, pp. 301–330.

Baker, C. and Young, R.P. (1997) Evidence for extensile crack initiation in point source time-dependent moment tensor solutions, Bull. Seismol. Soc. Am., 87, pp. 1442–1453.

Brodsky, E.E., Kanamori, H. and Sturtevant, B. (1999) A seismically constrained mass discharge rate for the initiation of the May 18, 1980 Mount St. Helens eruption, J. Geophys. Res., 104, pp. 29387–29400.

Burridge, R. and Knopoff, L. (1964) Body force equivalents for seismic dislocations, Bull. Seismol. Soc. Am., 54, pp. 1875–1888.

Dahlen, F.A. (1993) Single-force representation of shallow landslide sources, Bull. Seismol. Soc. Am., 83, pp. 130–143.

Eissler, H.K. and Kanamori, H. (1987) A single-force model for the 1975 Kalapana, Hawaii, earthquake, J. Geophys. Res., 92, pp. 4827–4836.

Feignier, B. and Young, R.P. (1992) Moment tensor inversion of induced microseismic events: Evidence of non-shear failures in the -4<M<-2 moment magnitude range, Geophys. Res. Lett., 19, pp. 1503–1506.

Ferreira, R. (2004) personal communication, Rock Mechanics Department, Driefontein Gold mine, Gold Fields, South Africa.

Frohlich, C. (1984) Earthquakes with non-double-couple mechanisms, Science, 264, pp. 804–809.

Hasegawa, H.S. and Kanamori, H. (1987) Source mechanism of the magnitude 7.2 Grand Banks earthquake of November 1929: Double couple or submarine landslide?, Bull. Seismol. Soc. Am., 77, pp. 1984–2004.

Hasegawa, H.S., Wetmiller, R.J. and Gendzwill, D.J. (1989) Induced seismicity in mines in Canada – An overview, Pure Appl. Geophys., 129, pp. 423–453.

Julian, B.R., Miller, A.D. and Foulger, G.R. (1998) Non-double-couple earthquakes. 1. Theory, Rev. Geophys., 36, pp. 525–549.

Kanamori, H. and Given, J.W. (1982) Analysis of long-period seismic waves excited by the May 18, 1980, eruption of Mount St. Helens – A terrestrial monopole, J. Geophys. Res., 87, pp. 5422–5432.

Kanamori, H., Given, J.W. and Lay, T. (1984) Analysis of seismic body waves excited by the Mount St. Helens eruption of May 18, 1980, J. Geophys. Res., 89, pp. 1856–1866.

Kawakatsu, H. (1989) Centroid single force inversion of seismic waves generated by landslides, J. Geophys. Res., 94, pp. 12363–12374.

Kuge, K. and Lay, T. (1994) Data-dependent non-double-couple components of shallow earthquake source mechanisms: effects of waveform inversion instability, Geophys. Res. Lett., 21, pp. 9–12.

McGarr, A. (1992) Moment tensors of ten Witwatersrand mine tremors. PAGEOPH, Vol. 139, No. 3/4, pp. 781–801.

Milev, A.M., Spottiwoode, S.M., Rorke, A.J. and Finnie, G.J. (2001) Seismic monitoring of a simulated rockburst on a wall of an underground tunnel, J. South Afr. Inst. Min. Metall., 101, pp. 253-260.

Miller, A.D., Foulger, and Julian, B.R. (1998) Non-double-couple earthquakes. 2. Observations, Rev. Geophys., 36, pp. 551-568.

Nishimura, T. (1995) Source parameters of the volcanic eruption earthquakes at Mount Tokachi, Hokkaido, Japan, and a magma ascending model, J. Geophys. Res., 100, 12465-12473.

Okal, E.A. (1990) Single forces and double-couples – a theoretical review of their relative efficiency for the excitation of seismic and tsunami waves, J. Phys. Earth, 38, pp. 445–474.

Rudajev, V. and Šílený, J. (1985) Seismic events with non-shear component II. Rock bursts with implosive source component, Pure Appl. Geophys., 123, pp. 17–25.

Šílený, J. (1998) Earthquake source parameters and their confidence regions by a genetic algorithm with a "memory", Geophys. J. Int., 134, pp. 228–242.

Šílený, J., Panza, G.F. and Campus, P. (1992) Waveform inversion for point source moment tensor retrieval with variable hypocentral depth and structural model, Geophys. J. Int., 109, pp. 259–274.

Šílený, J., Pšen ík, I. and Young, R.P. (2001) Point-source inversion neglecting nearby free surface: simulation of the Underground Research Laboratory, Canada. Geophys. J. Int., 146, pp. 171–180.

Šílený, J. and Vavry uk, V. (2000) Approximate retrieval of the point source in anisotropic media: numerical modelling by indirect parametrization of the source. Geophys. J. Int., 143, pp. 700–708.

Šílený, J. and Vavry uk, V. (2002) Can unbiased source be retrieved from anisotropic waveforms by using an isotropic model of the medium?, Tectonophysics, 356, pp. 125–138.

Sipkin, S.A. (1982) Estimation of earthquake source parameters by the inversion of waveform data: synthetic waveforms, Phys. Earth Planet. Inter., 30, pp. 242–259.

Stickney, M.C. and Sprenke, K.F. (1993) Seismic events with implosional focal mechanisms in the Couer d'Alene mining ditrict, northern Idaho, J. Geophys. Res., 98, pp. 6523–6528.

Takei, Y. and Kumazawa, M. (1994) Why have the single force and torque been excluded from seismic source models?, Geophys. J. Int., 118, pp. 20–30.

Takei, Y. and Kumazawa, M. (1995) Phenomenological representation and kinematics of general seismic sources including the seismic vector modes, Geophys. J. Int., 121, pp. 641–662.

Wong, I.G. and McGarr, A. (1990) Implosional failure in mining induced seismicity: A critical review, in Rockbursts and Seismicity in Mines, ed. C. Fairhurst, pp. 45-51. Balkema, Brookfield, Vt.

Wong, I.G., Humphrey, J.R., Adams, J.A. and Silva W.J. (1989) Observations of mine seismicity in the eastern Wasatch Plateau, Utah, USA: A possible case of implosional failure, Pure Appl. Geophys., 129, pp. 369–405.